nature cell biology

PML regulates p53 stability by sequestering Mdm2 to the nucleolus

Rosa Bernardi[1], Pier Paolo Scaglioni[1,3], Stephan Bergmann[1,3], Henning F. Horn[2], Karen H. Vousden[2] and Pier Paolo Pandolfi[1,4]

The promyelocytic leukaemia (PML) tumour-suppressor protein potentiates p53 function by regulating post-translational modifications, such as CBP-dependent acetylation[1,2] and Chk2-dependent phosphorylation, in the PML-Nuclear Body (NB)[3]. PML was recently shown to interact with the p53 ubiquitin-ligase Mdm2 (refs 4–6); however, the mechanism by which PML regulates Mdm2 remains unclear. Here, we show that PML enhances p53 stability by sequestering Mdm2 to the nucleolus. We found that after DNA damage, PML and Mdm2 accumulate in the nucleolus in an Arf-independent manner. In addition, we found that the nucleolar localization of PML is dependent on ATR activation and phosphorylation of PML by ATR. Notably, in *Pml*$^{-/-}$ cells, sequestration of Mdm2 to the nucleolus was impaired, as well as p53 stabilization and the induction of apoptosis. Furthermore, we demonstrate that PML physically associates with the nucleolar protein L11, and that L11 knockdown impairs the ability of PML to localize to nucleoli after DNA damage. These findings demonstrate an unexpected role of PML in the nucleolar network for tumour suppression.

The mechanisms promoting the up-regulation and transcriptional activation of p53 are critical for modulating its role in tumour suppression. The product of the *mdm2* proto-oncogene physically interacts with p53 and is a negative regulator of p53 in cells that are not subjected to stress. It does this by functioning as a p53 ubiquitin ligase[7]. Disruption of the p53–Mdm2 complex is achieved in several ways, such as phosphorylation of p53 or Mdm2 (or both) and sequestration of either p53 or Mdm2 to separate sub-nuclear compartments[7]. These mechanisms can be differentially utilized after distinct cellular stresses; for example, nucleolar sequestration of Mdm2 can occur after replicative senescence[8] or after inhibition of RNA polymerase I by actinomycin D (nucleolar stress)[9].

The *PML* gene encodes a tumour suppressor involved in the pathogenesis of acute promyelocytic leukemia (APL)[10]. The PML protein localizes to multi-protein sub-nuclear structures termed PML-NBs[11]. Numerous proteins associate dynamically with PML in PML-NBs after specific stimuli. In particular, after oncogenic stress and DNA damage induced by γ-irradiation, PML functions as a p53 transcriptional co-activator by recruiting it to the PML-NBs[1,2,12]. Here, it facilitates acetylation of p53 (on Lys-382), mediated by the acetyltransferase CBP[1,2]. However, we found that PML-IV (the PML isoform that binds p53; refs 2, 13) could function as a p53 transcriptional co-activator, even after substitution of critical p53 lysine residues with arginines ($p53^{K382R}$, $p53^{K320R}$ and $p53^{K5R}$ mutants; see Supplementary Information, Fig. S1). These results suggest that PML may potentiate p53 activity through additional mechanisms.

We reasoned that PML might directly influence p53 protein stability. Indeed, increasing amounts of PML induced the accumulation of p53 and p53 target genes, such as p21 (Fig. 1a), by increasing the half-life of p53 (Fig. 1b). Importantly, overexpression of PML in p53/Mdm2 double-null (*Mdm2*$^{-/-}$/*p53*$^{-/-}$) mouse embryonic fibroblasts (MEFs) did not result in the accumulation of transfected p53 (Fig. 1c), but prevented the reduction in p53 levels caused by cotransfection of human Mdm2 (Hdm2; Fig. 1d). These results demonstrate that PML can stabilize p53 by antagonizing Mdm2 function.

The stabilization of p53 in wild-type and *Pml*$^{-/-}$ primary cells was examined after the introduction of p53-dependent apoptotic stimuli. In *Pml*$^{-/-}$ MEFs, the accumulation of p53 after treatment with the topoisomerase inhibitor doxorubicin and the cross-linking agent mitomycin C was impaired (Fig. 1e). The phosphorylation of p53 on Ser 18 (Ser 15 in human p53) and acetylation on Lys 320 and Lys 382 paralleled the levels of total p53 in MEFs treated with doxorubicin and mitomycin C (see Supplementary Information, Fig. S2). This suggested that these p53 post-translational modifications were not defective; thus, they could not account for the defect in p53 accumulation that was observed in *Pml*$^{-/-}$ MEFs. As PML promoted p53 stabilization by counteracting the function of Mdm2, we reasoned that the absence of *Pml* might result in an increase in p53 ubiquitination after DNA damage. Wild-type and *Pml*$^{-/-}$ cells were transfected with haemagglutinin fused to ubiquitin (HA–Ub) and treated with doxorubicin, as well as the proteasome inhibitor MG132 (to prevent p53 degradation). Immunoprecipitation of endogenous p53 identified a marked increase in p53–HA–Ub complexes in *Pml*$^{-/-}$, cells compared with wild-type cells (Fig. 1f). Therefore, after DNA damage in *Pml*$^{-/-}$ cells, p53 stability is impaired and p53 ubiquitination increases. Interestingly, wild-type MEFs treated with doxorubicin and mitomycin C showed a significant up-regulation of *Pml*, which

[1]Cancer Biology and Genetics Program, Department of Pathology and Medicine, Sloan-Kettering Institute, Memorial Sloan-Kettering Cancer Center, New York, NY 10021, USA. [2]Beatson Institute for Cancer Research, Glasgow G61 1BD, UK. [3]These authors contributed equally to this work.
[4]Correspondence should be addressed to P.P.P. (e-mail: p-pandolfi@ski.mskcc.org)

Published online: 13 June 2004, DOI: 10.1038/ncb1147

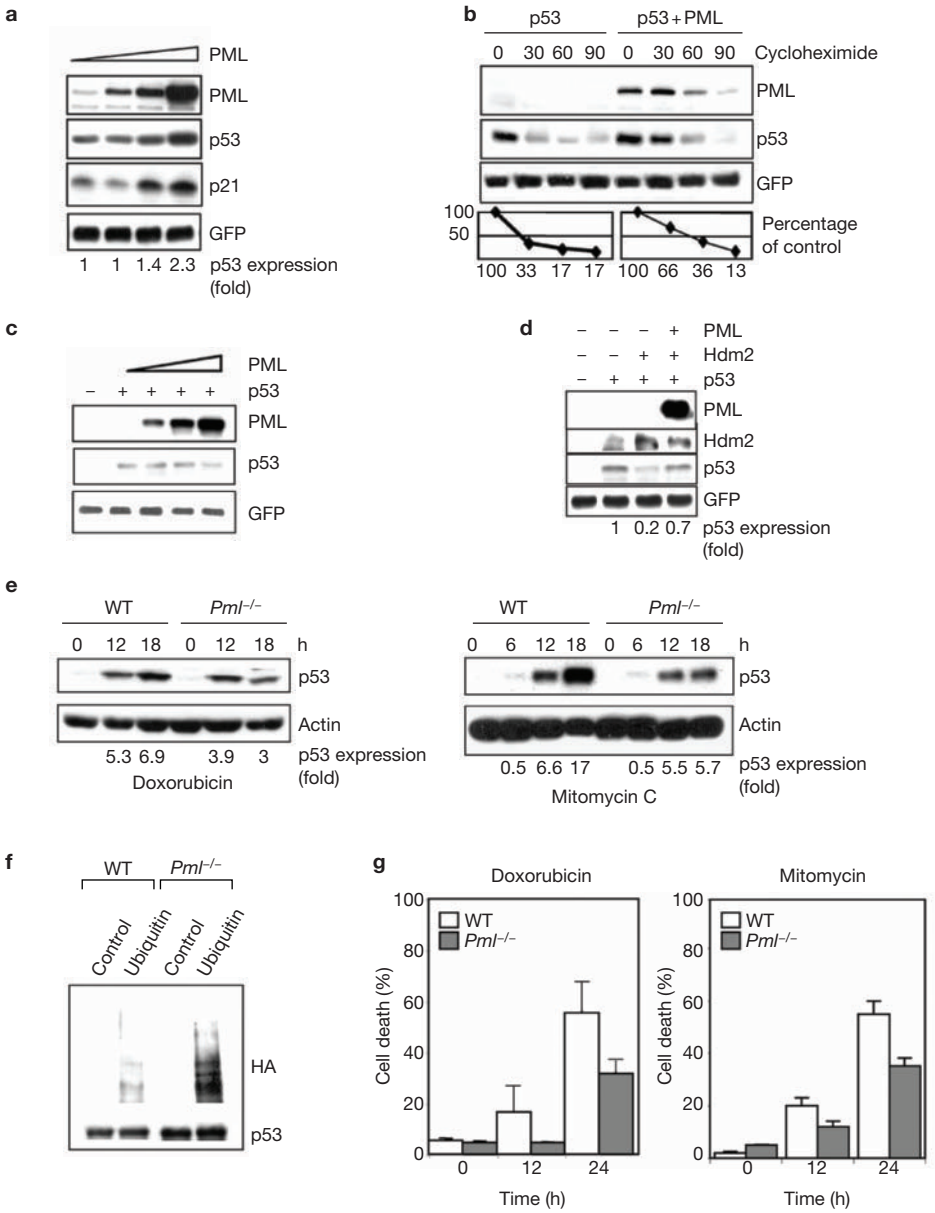

Figure 1 PML mediates stabilization of p53 in the presence of Mdm2. (**a**) Western blot analysis of H1299 cells transfected with p53 and increasing amounts of PML-IV. pEGFP was cotransfected to monitor transfection efficiency. Intensity of the bands quantified by densitometry is expressed as p53 expression (fold) over the levels of p53 alone. (**b**) p53, pEGFP and PML-IV were transfected in H1299 cells as indicated. At 24 h after transfection, cells were incubated with cycloheximide for the indicated times and analysed by western blotting. p53 protein levels were assessed by densitometry. (**c**) *Mdm2*$^{-/-}$/*p53*$^{-/-}$ MEFs were transfected as in **a** and were analysed by western blotting. (**d**) Western blot analysis of *Mdm2*$^{-/-}$/*p53*$^{-/-}$ MEFs after transfection with the indicated plasmids. (**e**) Wild-type and *Pml*$^{-/-}$ MEFs were treated with doxorubicin and mitomycin C for the indicated times. Cell lysates were analysed by western blotting. p53 protein levels, relative to untreated cells and to actin levels, are indicated at the bottom of the panels. (**f**) Wild-type and *Pml*$^{-/-}$ immortalized MEFs were transfected with control vector or HA–Ub and pEGFP. At 24 h after transfection, cells were treated with doxorubicin for 12 h and with MG132 for the last 6 h. p53 was immunoprecipitated and the western blot was probed with anti-HA and anti-p53 antibodies. (**g**) Wild-type (white bars) and *Pml*$^{-/-}$ (grey bars) MEFs were treated for 12 and 24 h with doxorubicin (left) or mitomycin C (right). Cell viability was measured by trypan blue exclusion. All panels (**a**–**g**) are representative of at least three independent experiments.

coincided with the accumulation of p53 (see Supplementary Information, Fig. S2). Notably, doxorubicin- and mitomycin-C-induced apoptosis was markedly impaired in the absence of *Pml* (Fig. 1g). Therefore, PML is important for the accumulation of p53 and the induction of apoptosis after DNA damage.

To understand the mechanisms underlying p53 stabilization by PML, we analysed the localization of PML, Mdm2 and p53 after DNA damage. Surprisingly, in WI38 (normal human embryonic fibroblasts) cells and wild-type MEFs treated with doxorubicin, PML concentrated in the nucleoli, as demonstrated by co-localization with nucleolar markers (Fig. 2a, b). In the majority of cells, PML accumulated at the periphery of the nucleolus. Accumulation of PML in the nucleolus was not accompanied by a disappearance of the PML-NBs, and this accumulation was also observed after mitomycin C treatment (data not

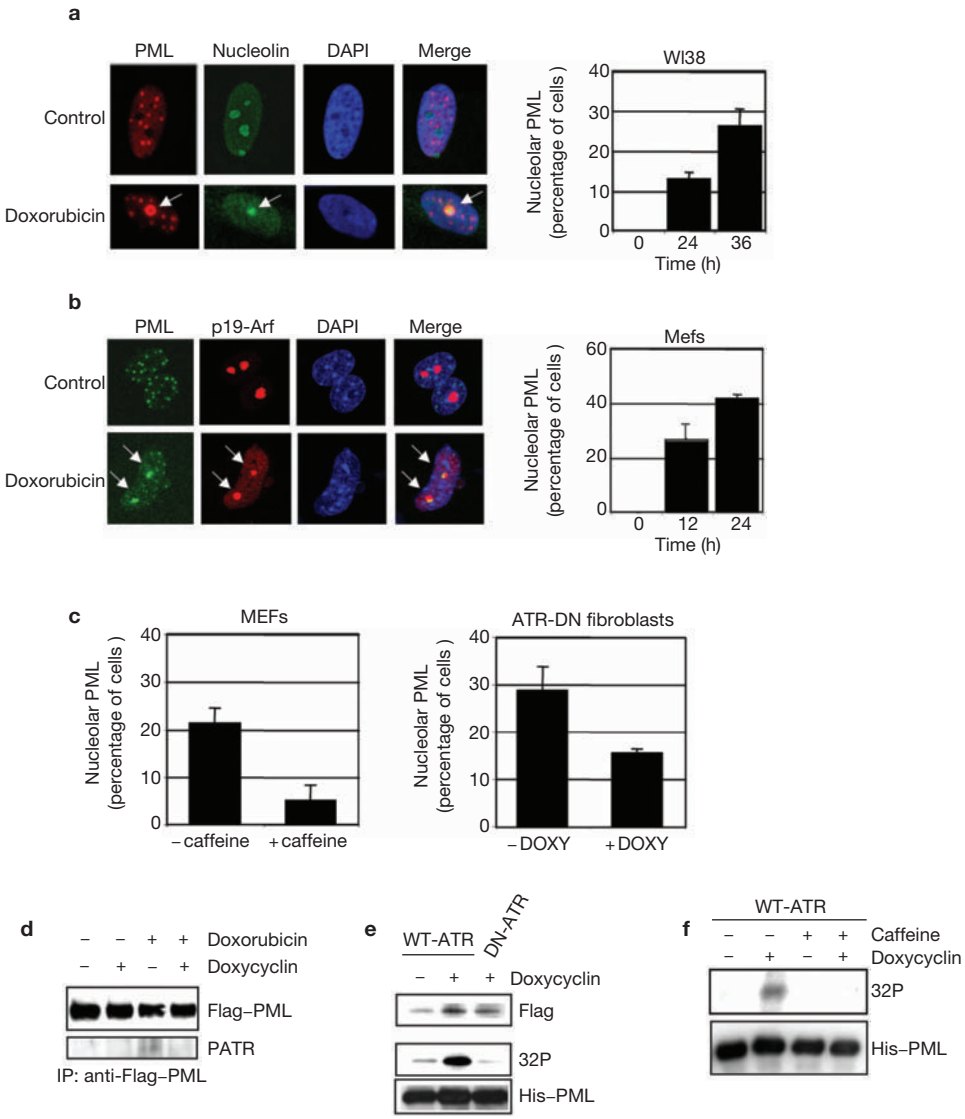

Figure 2 PML accumulates in the nucleolus and is phosphorylated by ATR after DNA damage. WI38 human fibroblasts (**a**) and MEFs (**b**) were cultured for 36 and 24 h, respectively, in the presence of doxorubicin. Both PML and nucleolin (**a**), and PML and p19-Arf (**b**), were detected by indirect immunofluorescence microscopy. Cell nuclei were visualized with DAPI (blue). Fields were merged to assess protein colocalization. Upper panels show control cells, bottom panels show cells treated with doxorubicin. Graphs to the right show the percentage of cells displaying PML nucleolar staining after treatment with doxorubicin. (**c**) Left, MEFs treated with doxorubicin in the presence of absence of caffeine for 12 h. Right, ATR-DN fibroblasts treated with doxorubicin in the presence of absence of doxycycline for 12 h. In both panels, an average of 300 cells were scored for nucleolar PML. The panels represent four independent experiments. (**d**) ATR-DN fibroblasts were transfected with PML-IV. At 24 h after transfection, cells were treated with doxorubicin and doxycycline, as indicated, for 12 h. PML was immunoprecipitated with an anti-Flag antibody. Western blot analysis was performed with an anti-P-ATR antibody and subsequently with an anti-Flag antibody. (**e**) ATR kinase assay with purified His–PML. U2OS cells expressing inducible Flag–WT-ATR or Flag–ATR-DN were treated with doxycycline for 48 h. Anti-Flag immunoprecipitates were incubated with His–PML in the presence of ^{32}P-ATP. Kinase reactions were analysed by autoradiography and by western blotting with anti-Flag and anti-His antibodies to measure protein levels. (**f**) Wild-type ATR was immunoprecipitated as in **e**. Kinase assays were performed with or without caffeine. Panels **c**–**f** are representative of three independent experiments.

shown). Six hours after doxorubicin treatment, nucleoli could not be detected by immunofluorescence microscopy with nucleolar markers (data not shown), as noted after other cellular stresses[14]. However, nucleoli reformed at later times (onwards of 12 h), when PML was found to colocalize with nucleolar proteins (Fig. 2a, b). SUMO-1 localized to the nucleolus with PML after doxorubicin treatment (data not shown), suggesting that nucleolar PML may be SUMO-modified.

ATM and ATR kinases are the major regulators of a cascade of cellular responses to DNA damage that result in either cell-cycle arrest and DNA repair or apoptosis[15]. Therefore, we tested whether PML accumulation in the nucleolus was part of an ATM- or ATR-dependent checkpoint response. A dose of caffeine that is known to inhibit both ATM and ATR[16] markedly blocked the localization of PML to the nucleolus after doxorubicin treatment (Fig. 2c, left panel). To determine whether PML localization was dependent on the function of ATM, ATR, or both, *Atm*$^{-/-}$ primary cells were used[17]. PML localization in the nucleolus was unaffected by *Atm* inactivation (data not shown). A human cell line stably transfected with a

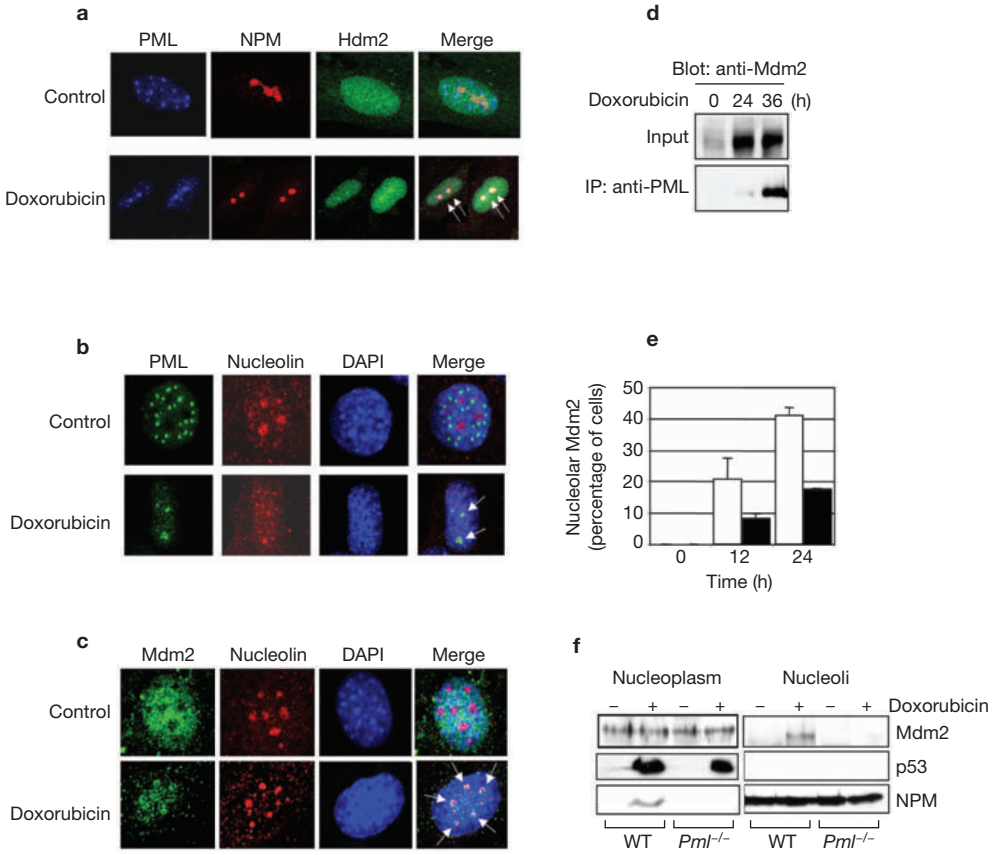

Figure 3 Mdm2 and PML colocalize in the nucleolus after DNA damage. (**a**) Triple staining of PML, NPM and Hdm2 in WI38 cells treated with doxorubicin for 36 h. Cells were stained with anti-PML (blue), anti-NPM (red) and anti-Hdm2 (green) antibodies and analysed by confocal microscopy. (**b**, **c**) PML and Mdm2 localize to the nucleolus in *Arf*$^{-/-}$ MEFs treated with doxorubicin. 18 h after treatment, cells were stained with anti-PML antibody (green), anti-nucleolin antibody (red) (**b**), anti-Mdm2 antibody (green) and anti-nucleolin antibody (red) (**c**) before analysis by confocal immunofluorescence microscopy. Nuclei were stained with DAPI (blue). (**d**) Extracts of WI38 cells treated for 24 or 36 h with doxorubicin were immunoprecipitated with anti-PML antibody. The input was 5% of that used in the immunoprecipitation (top). Western blot analysis was carried out with an anti-Mdm2 antibody. The panel is representative of two independent experiments. (**e**, **f**) Mdm2 nucleolar accumulation is impaired in *Pml*$^{-/-}$ cells. (**e**) Graphic representation of the percentage of wild-type (white columns) and *Pml*$^{-/-}$ MEFs (black columns) displaying nucleolar Mdm2 staining after incubation with doxorubicin for 12 and 24 h. More than 400 cells were analysed by confocal immunofluorescence microscopy in three independent experiments. (**f**) Western blot analysis of Mdm2, NPM and p53 from nucleoplasmic and nucleolar extracts of wild-type and *Pml*$^{-/-}$ MEFs treated with doxorubicin for 12 h.

tetracycline-inducible dominant-negative form of ATR (ATR-DN; see Methods) was then used[18]. Induction of ATR-DN by doxycycline significantly reduced the accumulation of PML in the nucleolus after doxorubicin treatment (Fig. 2c, right). Endogenous PML immunoprecipitated from doxorubicin-treated wild-type MEFs, was recognized with an antibody against proteins phosphorylated by ATM or ATR (data not shown). In addition, PML was overexpressed in ATR-DN fibroblasts treated with doxorubicin in the presence or absence of doxycycline. Immunoprecipitated PML was recognized by the anti-phospho-ATM/ATR antibody, but only after treatment with doxorubicin and in the absence of doxycycline (Fig. 2d). Finally, ATR kinase assays were performed with purified His-tagged PML (His–PML) and cell extracts from U2OS cells expressing inducible wild-type or dominant-negative ATR[19]. PML was phosphorylated after induction of wild-type, but not dominant-negative, ATR (Fig. 2e). Furthermore, this phosphorylation was inhibited by caffeine (Fig. 2f), demonstrating that PML is a direct target of ATR. In conclusion, PML is phosphorylated and accumulates in the nucleolus after DNA damage as part of a checkpoint response that depends on ATR activation.

The localization of Mdm2 and p53 after DNA damage was examined. Mdm2 accumulated in the nucleolus after doxorubicin treatment and colocalized with nucleolar PML, as shown by triple-staining of Hdm2, PML and nucleophosmin (NPM; Fig. 3a). Importantly, nucleolar localization of both PML and Mdm2 after doxorubicin treatment also occurred in *Arf*$^{-/-}$ MEFs (Fig. 3b, c). Furthermore, endogenous PML and Mdm2 were coimmunoprecipitated from WI38 cells after DNA damage at times when they were found to colocalize in the nucleolus (Fig. 3d; also see Fig. 2a). In contrast, p53 did not accumulate in the nucleolus after doxorubicin treatment (data not shown). Together, these data demonstrate that after DNA damage, Mdm2 is sequestered in the nucleolus in an ARF-independent manner, where it interacts with PML.

Therefore, we tested whether sequestration of Mdm2 to the nucleolus after DNA damage was PML-dependent. The percentage of *Pml*$^{-/-}$ MEFs displaying nucleolar Mdm2 after doxorubicin treatment was markedly reduced when compared with wild-type MEFs (Fig. 3e). To further quantify these differences, nucleoli were isolated from wild-type and *Pml*$^{-/-}$ MEFs before and after doxorubicin treatment. Mdm2 was found in the nucleoplasm of both wild-type and *Pml*$^{-/-}$ cells (Fig. 3f).

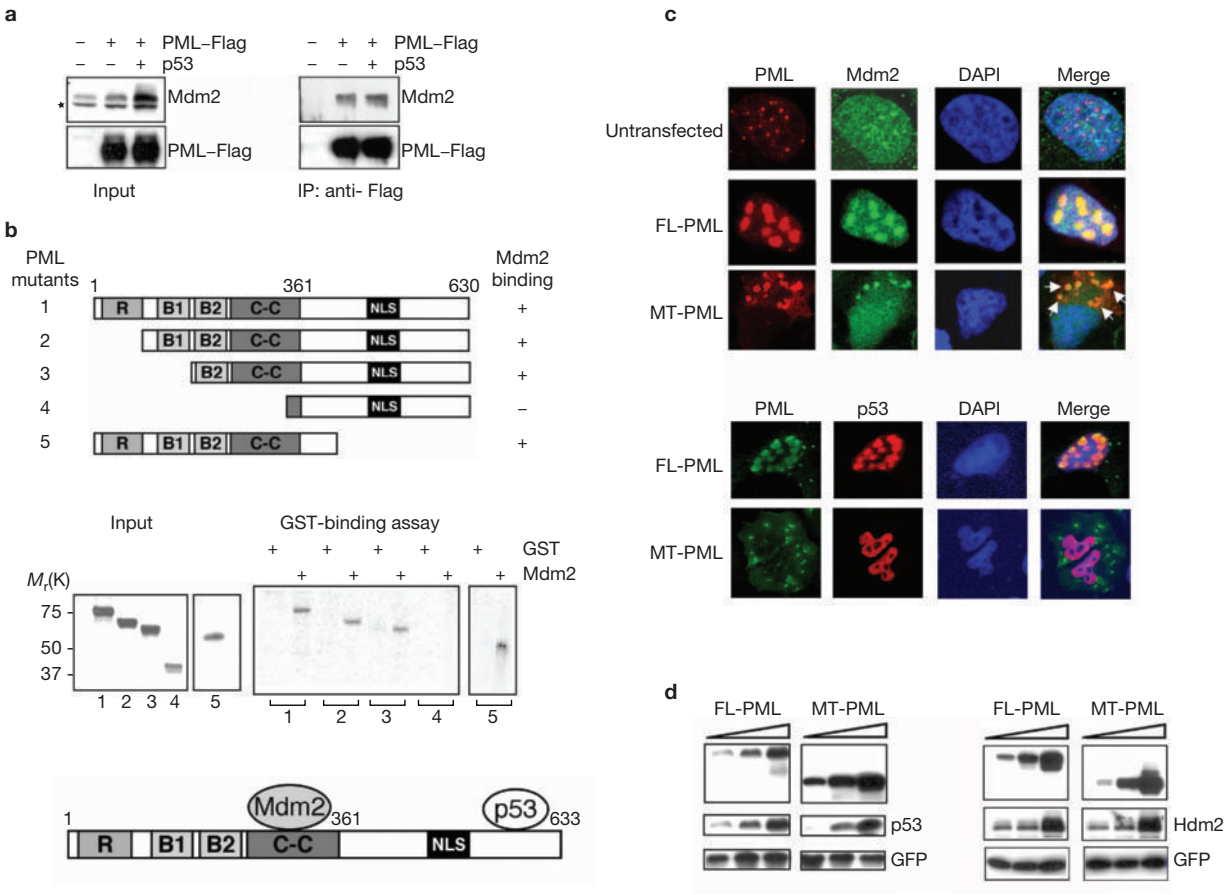

Figure 4 PML interacts directly with Mdm2 and stabilizes p53 through sequestration of Mdm2. (**a**) H1299 cells were transfected with PML-IV and p53 as indicated. 48 h after transfection, cell extracts were immunoprecipitated with an anti-Flag antibody (right). Cell lysates were loaded as a control (left). Western blot analysis was performed with anti-Flag and anti-Mdm2 antibodies as indicated. The asterisk indicates a non-specific band. The panel is representative of three independent experiments. (**b**) GST-binding assay with GST–Mdm2 and *in vitro*-translated PML. ^{35}S-labelled full-length PML-IV (indicated as 1) and deletion mutants of PML-IV (indicated as 2–5) were incubated with GST or GST–Mdm2. The input represents 50% of what was used in the assay. A schematic representation of p53- and Mdm2-binding regions of PML is displayed at the bottom. (**c**) Upper panels, H1299 cells were left untransfected or transfected with full-length PML-IV (FL-PML) and PML mutant 5 (MT-PML) and analysed by immunofluorescence microscopy with anti-PML (red) and anti-Mdm2 (green) antibodies. Nuclei are stained with DAPI (blue). Arrows indicate colocalization of Mdm2 and MT-PML in the cytoplasm. Lower panels, H1299 cells transfected with FL-PML or MT-PML, as well as p53, were analysed by immunofluorescence microscopy with anti-PML (green) and anti-p53 (red) antibodies. Nuclei are stained with DAPI (blue). (**d**) Western blot analysis of H1299 cell lysates 24 h after transfection with p53 (left panel) or Hdm2 (right panel), as well as increasing amounts of FL-PML and MT-PML. pEGFP was cotransfected to monitor transfection efficiency. The panels are representative of three independent experiments.

However, after doxorubicin treatment, a percentage of Mdm2 could be detected in the nucleolar fraction of wild-type cells, but not *Pml*$^{-/-}$ cells (Fig. 3f). These findings demonstrate that PML is critical for nucleolar accumulation of Mdm2 after DNA damage.

Our data imply that PML may promote p53 stabilization by sequestering Mdm2. To test this hypothesis, we assessed whether PML and Mdm2 interact directly and, if so, whether a mutant of PML that binds Mdm2, but not p53, stabilizes p53. PML and Mdm2 interacted in p53-null H1299 cells, even in the absence of p53 (Fig. 4a). Glutathione *S*-transferase (GST) pull-down assays with GST or GST–Mdm2, as well as deletion mutants of PML, demonstrated that the two proteins interact directly. The binding site for Mdm2 resided around the coiled-coil motif of PML, which is shared by all PML isoforms (Fig. 4b). p53, however, binds to the extreme carboxyl terminus of PML-IV[13] (Fig. 4b). Next, a PML mutant (PML mutant 5 in Fig. 4b; MT-PML) that binds Mdm2, but not p53, was examined. This mutant lacks the nuclear localization signal (NLS) and forms cytoplasmic aggregates when overexpressed (Fig. 4c). MT-PML was used in these experiments (rather than other PML isoforms), because all PML isoforms have been reported to recruit p53 to the PML-NB[20]. MT-PML recruited endogenous Mdm2 to the cytoplasm (Fig. 4c, top), but failed to recruit cotransfected p53 (Fig. 4c, bottom). Similar results were obtained with *Pml*$^{-/-}$ MEFs (data not shown). Notably, MT-PML stabilized p53 to the same extent as full-length PML (FL-PML; Fig. 4d, left). Interestingly, both FL-PML and MT-PML promoted the accumulation of Hdm2 (Fig. 4d, right), suggesting that PML can inhibit Hdm2 self-ubiquitination/degradation, as previously shown for ARF[21] and the ribosomal protein L11 (ref. 9). Together, these results suggest that PML can promote accumulation of p53 by sequestering Mdm2 in the absence of direct PML/p53 binding.

During replicative senescence, the tumour-suppressor protein ARF binds to Mdm2 and sequesters it in the nucleolus[8]. Nucleolar

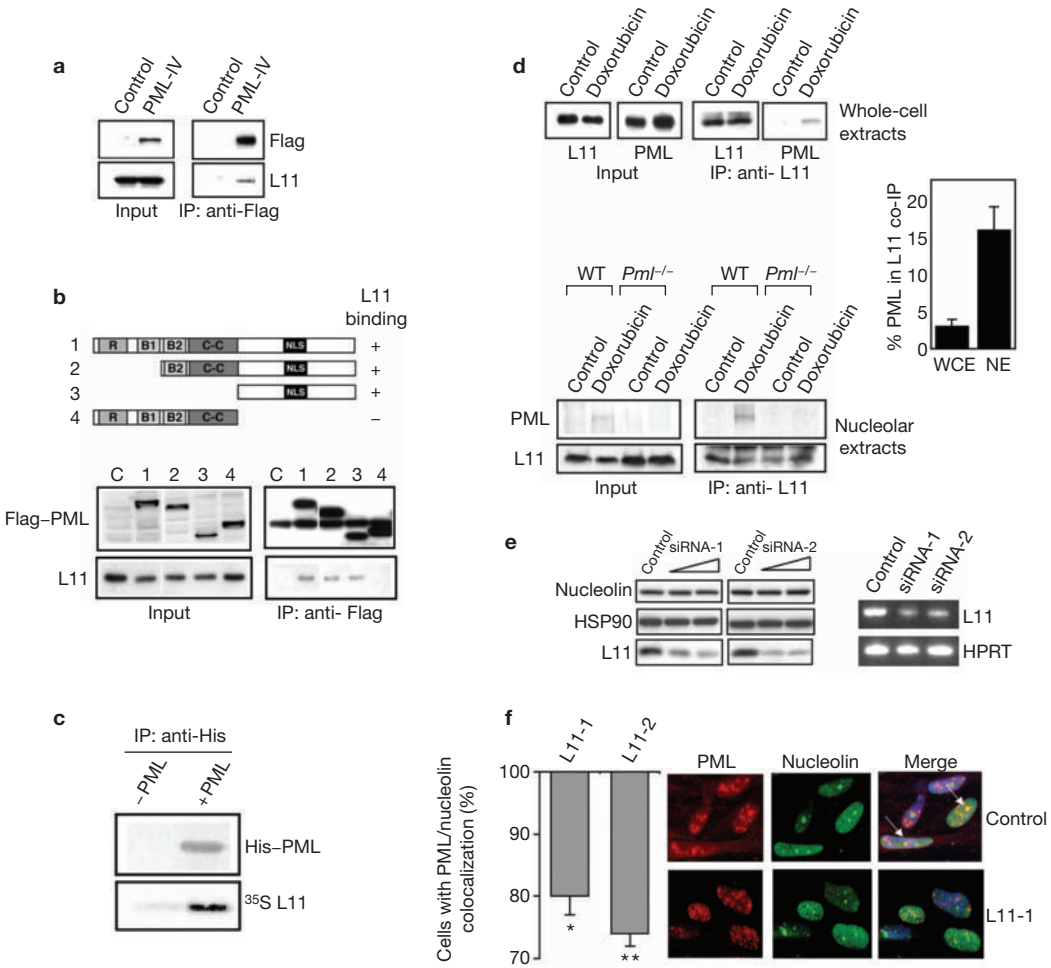

Figure 5 L11 facilitates PML nucleolar localization after DNA damage. (**a**) NIH 3T3 cells transfected with control vector or PML-IV were immunoprecipitated with an anti-Flag antibody. Western blot analysis was performed with anti-Flag and anti-L11 antibodies. (**b**) H1299 cells were transfected with full-length and mutant PML proteins, which were then immunoprecipitated with anti-Flag antibody. Western blot analysis was performed with anti-Flag and anti-L11 antibodies. (**c**) *In-vitro*-translated L11 was incubated with anti-His antibody with or without affinity-purified His–PML. The complex was resolved by SDS–PAGE, stained with Coomassie blue and analysed by autoradiography. (**d**) Top, whole-cell extracts from immortalized wild-type MEFs treated for 18 h with doxorubicin were immunoprecipitated with an anti-L11 antibody. Western blot analysis was performed with anti-PML and anti-L11 antibodies. Panels are representative of four independent experiments. Bottom, nucleolar extracts from wild-type and *Pml*$^{-/-}$ MEFs were immunoprecipitated with an anti-L11 antibody. Panels are representative of two independent experiments. Inputs are 5–10% of that used in the immunoprecipitations. The graph indicates the amount of PML co-immunoprecipitated with L11 as a percentage of the total amount of PML in inputs. WCE, whole-cell extracts; NE, nucleolar extracts. (**e**) WI38 cells were transfected with control siRNA or increasing amounts of L11-specific siRNA-1 and siRNAi-2. At 48 h after transfection, western blot analysis for nucleolin, HSP90 and L11 (left) and RT–PCR for L11 and HPRT for normalization (right) were performed. (**f**) WI38 cells were transfected with control or L11 siRNA-1 and siRNAi-2 for 48 h and treated with doxorubicin for the last 36 h. Cells were stained with anti-nucleolin and anti-PML antibodies. The graph expresses the percentage of cells with nucleolin-PML colocalization in L11 siRNA-transfected samples versus control siRNA-transfected cells (control oligonucleotide-treated cells = 100%; $^{*}P = 0.02$; $^{**}P = 0.003$). Data is representative of three independent experiments.

localization of Mdm2 after actinomycin D treatment, however, is ARF-independent and is mediated by the nucleolar protein L11 (ref. 9). Actinomycin D treatment also induced the localization of PML to the nucleolus (data not shown). Therefore, we hypothesized that both Mdm2 and PML might interact with L11 after DNA damage, and that L11 might mediate nucleolar localization of PML. Endogenous L11 co-immunoprecipitated with overexpressed PML in NIH 3T3 fibroblasts (Fig. 5a) and H1299 cells (data not shown). PML deletion mutants that lacked the C-terminal region could no longer interact with L11 (Fig. 5b), suggesting that L11 binding does not overlap with the Mdm2-binding region (Fig. 4b). *In vitro* binding assays demonstrated that PML and L11 can interact directly (Fig. 5c). Thus, we reasoned that endogenous PML and L11 might interact in the nucleolus after doxorubicin treatment. Low levels of PML were co-immunoprecipitated with an anti-L11 antibody in wild-type MEFs after doxorubicin treatment (Fig. 5d, top). Importantly, the amount of PML from isolated nucleoli that co-immunoprecipitated with L11 was considerably higher than that from whole-cell extracts (Fig. 5d, compare bottom and top panels, and see graph). Thus PML and L11 interact specifically in the nucleoli.

Next, we assessed whether L11 is required for the nucleolar accumulation of PML. Small-interfering RNAs (siRNAs) knocked-down L11 expression in WI38 cells. Two siRNAs were tested, and both produced similar reductions in L11 expression (up to 50%), while leaving other

nucleolar proteins unaffected (Fig. 5e). PML nucleolar localization was analysed in cells treated with control siRNAs or L11 siRNAs after doxorubicin treatment. The number of cells displaying colocalization of PML with nucleolin (or NPM; data not shown) was reduced markedly in L11 siRNA-treated cells (Fig. 5f). As L11 interacts with Mdm2 after treatment with actinomycin D[9,22], we reasoned that Mdm2 and L11 might also interact after doxorubicin treatment; furthermore, PML might be required for this interaction. Overexpressed Mdm2 and L11 co-immunoprecipitated from both wild-type and *Pml*$^{-/-}$ cells; however, doxorubicin treatment only increased this interaction in the presence of PML (see Supplementary Information, Fig. S3). Together, these results demonstrate that PML interacts with L11 in the nucleolus and that this interaction is important for the localization of PML to the nucleolus.

Our analysis leads to three major conclusions. First, PML (until now considered to be a NB protein) can be found in a distinct subcellular compartment (the nucleolus) after cellular stress. It is important to note that PML accumulates in the nucleolus after treatment with specific DNA-damaging agents (for example, doxorubicin, but not γ-irradiation[23]; see Supplementary Information, Fig. S4). The nucleolar localization of PML is triggered by activation of the checkpoint kinase ATR, consistent with ATR activation being a major event in the induction of S/G2 checkpoints after exposure to topoisomerase inhibitors[24]. This observation, along with the finding that PML is a direct target of Chk2 phosphorylation after γ-irradiation[25], suggests that the localization and function of PML are regulated by different checkpoints in response to distinct apoptotic stimuli. Second, the accumulation of PML in the nucleolus is ARF-independent and, at least in part, dependent on the nucleolar protein L11. As nucleolar accumulation of PML is reduced but not abrogated after L11 knockdown, this suggests that other proteins may also function to dock PML at the nucleolus. Finally, PML is required for Mdm2 nucleolar localization and, in turn, p53 stabilization after DNA damage. As L11 can interact directly with Mdm2 and PML, it is possible that both proteins participate in a larger nucleolar complex to induce Mdm2 sequestration. Our data add complexity to the original working model by which PML regulates p53 function in the NB, and the PML-NB represents a site for modification and activation of p53 (refs 26, 27). □

METHODS

Cell culture. MEFs were prepared from embryos at day 13.5 of development (E13.5). Early passage (3–5) MEFs were used in all experiments, except as indicated. Wild-type and *Pml*$^{-/-}$ MEFs were immortalized using a 3T9 protocol and maintained in culture up to passage 30. p53 function was considered normal, as the protein was induced by doxorubicin treatment and cells displayed sensitivity to doxorubicin. H1299, NIH 3T3, 293T and WI38 cells were obtained from the American Type Culture Collection. The GM847 ATR-DN (dominant negative) cell line — an SV40-immortalized human fibroblast line expressing the ATR dominant-negative kinase under the control of a tetracycline-inducible system — was kindly provided by W. Cliby[17]. U2OS wild-type ATR and ATR-DN were kindly provided by S. Schreiber[18]. Induction of wild-type ATR and ATR-DN was achieved by 48-h-treatment with 1 μM doxycycline (Sigma, Saint Louis, MO). The *Atm*-null cell line 743 was a kind gift from M. Turker[16]. G. Lozano and M. van Lohuizen kindly provided *mdm2*$^{-/-}$/*p53*$^{-/-}$ and *Arf*$^{-/-}$ MEFs, respectively. Primary and established cells were cultured in DMEM supplemented with 10% foetal bovine serum, 4.5 mg ml^{-1} glucose and L-glutamine. Cells were treated with 0.5–2 μM doxorubicin depending on the sensitivity of the cell type (0.5–1 μM for MEFs or immortalized MEFs; 2 μM for WI38 cells; 1 μM for NIH3T3 cells; 1 μM for *Atm*-null cells; and 1 μM for ATR-DN cells) and 50 mg ml^{-1} mitomycin C, (Sigma). Cycloheximide and caffeine (Sigma) were used at 25 μM and 4 mM, respectively, for the indicated times. MG132 (Calbiochem, La Jolla, CA) was used at 10 μM.

Plasmids, cell transfection and transactivation assays. pCMV-Tag2B–PML-IV expresses PML isoform IV under the control of the CMV promoter. pCMV–WT-p53 and pCMV–p53^{K5R} (a p53 mutant in which lysines 370, 372, 373, 381 and 382 are substituted by arginines) expression vectors were a generous gift from W. Gu. PCMV–p53^{K320R} and pCMV–p53^{K382R} were created by site-directed mutagenesis to introduce a Lys–Arg substitution at position 320 or 382, respectively. PML-deletion mutants were as described[2], except for mutant 5, which was created by site-directed mutagenesis. CMV–Hdm2 was a gift from G. Lozano. pBax–luc, p21–luc and pMDM2–luc reporter plasmids were a kind gift from C. Di Como and C. Prives. GST–Mdm2 was from A. Weismann. His–PML was created by cloning PML-IV into pET-33b (Novagen, Madison, WI). Transient transfections were performed with the Effectene transfection reagent (Qiagen, Valencia, CA) according to the manufacturer's protocol. For transfections in H1299 cells, 50 ng of p53 were cotransfected with 50, 100 and 500 ng of PML-IV, with or without 500 ng of Hdm2. pEGFP (100 ng) or renilla- (50 ng) expressing plasmids were cotransfected to normalize for transfection efficiency. For transactivation assays, 200 ng of reporter plasmid was used and luciferase activity was assayed 24 h post-transfection. For Mdm2–L11 interaction, wild-type and *Pml*$^{-/-}$ immortalized MEFs were transfected with 2 μg CMV–Mdm2 and 4 μg CMV–L11. 24 h post-transfection, cells were treated with 1 μM doxorubicin for 18 h.

Western blotting, immunoprecipitation, *in vitro* protein interactions and ATR kinase assay. For western blot analysis, cells were lysed in ice-cold RIPA buffer containing a complete protease inhibitor cocktail (Boehringer Mannheim, Mannheim, Germany). Lysates were centrifuged to clear cell debris and 20–40 μg of lysate was used for analysis. The following antibodies were used: anti-human-p53 (DO-1; Santa Cruz, Santa Cruz, CA), anti-mouse-p53 (CM5; Novocastra, Newcastle, UK), anti-phospo-p53 (Ser 15; New England Biolabs, Beverly, MA), anti-Flag-M2 (Sigma), anti-Mdm2 (SMP14; Santa Cruz), anti-human-PML (PG-M3; Santa Cruz), rabbit anti-PML (kindly provided by K. S. Chang), anti-mouse PML (S36 and S37 monoclonal antibodies; kindly provided by S. Lowe), anti-GFP (Clontech, Palo Alto, CA), anti phospho-Ser/Thr-ATM/ATR (Cell Signaling, Beverly, MA) and anti-HA (Covance, Berkeley, CA). For co-immunoprecipitation, cells were lysed in immunoprecipitation (IP) buffer (150 mM NaCl, 50 mM Tris-HCl at pH 7.5 and 1% NP-40), supplemented with a complete protease-inhibitor cocktail. The lysate was precleared by incubation with protein-G– or protein-A–Sepharose beads (Amersham Biosciences, Piscataway, NY) and incubated with anti-Flag antibody, anti-human PML antibody (PG-M3) or anti-L11 antibody[9] overnight at 4°C before incubation with protein-G– or protein-A–Sepharose for 1 h. Immunoprecipitates were washed five times with ice-cold IP buffer and resolved by SDS–PAGE. Western blotting was performed according to standard procedures. For GST pull-down assays, *in vitro*-translated products were generated using the TNT Coupled System (Promega, Madison, WI). ^{35}S-labelled wild-type PML and PML mutants were incubated with GST and GST–Mdm2 in IP buffer for 2 h at 4°C. Beads were washed five times with IP buffer, and proteins were eluted with SDS sample buffer and resolved by SDS–PAGE before autoradiography. For ATR kinase assays, U2OS cells expressing wild-type ATR or ATR-DN were treated with doxycyclin for 48 h and ATR was immunoprecipitated from 2 mg of cell extract with anti-Flag antibody. Kinase assays were performed as previously described[18] with 1 μg purified His-PML as a substrate. Proteins were separated by SDS–PAGE, transferred onto membranes and exposed for autoradiography, as well as western blot analysis with an anti-Flag antibody.

Isolation of nucleoli. Nucleoli were prepared from wild-type and *Pml*$^{-/-}$ immortalized MEFs grown on 10 × 14 cm plates, as described[28]. Isolated nucleoli were resuspended in RIPA buffer and centrifuged at 13,000*g* to eliminate insoluble material. For L11–PML coimmunoprecipitations, nucleoli were resuspended in IP buffer and immunoprecipitated with anti-L11 antibody.

Immunofluorescence and confocal microscopy. Cells were grown on coverslips and treated as indicated. Cells were fixed in 4% paraformaldehyde for 10 min before permeabilization in PBS containing 0.1% Triton X-100 for 2 min. The antibodies used for immunofluorescence microscopy were: anti-human PML (PG-M3; Santa Cruz), anti-mouse PML (S36 and S37 monoclonal antibodies), anti-Mdm2 (SMP14; Santa Cruz), anti-nucleolin (4E2; Research Diagnostics,

Flanders, NJ), anti-p19^{Arf} (R562; Abcam, Cambridge, MA), anti-p53 (Ab-3; Oncogene Research Products, Darmstadt, Germany). Double staining was performed as indicated. For detection, cells were incubated with FITC-conjugated anti-mouse antibodies and Cy5-conjugated anti-rabbit antibodies (Jackson ImmunoResearch Laboratories, West Grove, PA). For triple staining, the antibodies used were: rabbit anti-PML (kindly provided by K. S. Chang), mouse anti-Mdm2 (SMP14; Santa Cruz) and goat anti-B23 (C-19; Santa Cruz). The secondary antibodies used for triple staining were: Alexa Fluor-405 anti-rabbit, Alexa Fluor-488 anti-mouse and Cy5-conjugated anti-goat (Molecular Probes, Eugene, OR). Slides were analysed by confocal microscopy.

L11 siRNA. siRNA oligonucleotides for L11 were obtained from Dharmacon (Lafayette, CO) in 2′-deprotected, annealed and desalted duplex form. The target sequences were nucleotides 198–218 (siRNA-1) and 262–282 (siRNA-2). WI38 cells were transfected with Lipofectamine 2000 (Invitrogen, Carlsbad, CA) according to the manufacturer's protocol. Cells were treated with doxorubicin 12 h after siRNA-transfection, fixed and analysed 36 h after treatment. Primers for L11 RT–PCR analysis were: 5′-GCGCAGGATCAAGGTGAA-3′; 5′-TTATTTCGGAGGAAGGAT-3′.

Note: Supplementary Information is available on the Nature Cell Biology website.

ACKNOWLEDGEMENTS

We are indebted to I. Guernah, A. Guo, P. Salomoni, F. Bernassola, and S. Grisendi for suggestions during the course of this work and critical reading of the manuscript. We are grateful to W. Cliby, C. Di Como, W. Gu, A. Levine, S. Lowe, G. Lozano, C. Prives, S. Schreiber, M. Turker, M. van Lohuizen and A. Weismann for reagents and advice. We thank Y. Haupt for useful discussion. R.B. and P.P.S. were supported by T32 training grants from the National Institutes of Health. P.P.S. is also a recipient of an ASCO Young Investigator Award and a CALGB Oncology Fellows Award. This work was supported by the award of a National Institutes of Health grant RO1 CA-71692 to P.P.P.

COMPETING FINANCIAL INTERESTS

The authors declare that they have no competing financial interests.

Received 30 November 2003; accepted 25 May 2004
Published online at http://www.nature.com/naturecellbiology.

1. Pearson, M. *et al.* PML regulates p53 acetylation and premature senescence induced by oncogenic *Ras*. *Nature* **406,** 207–210 (2000).
2. Guo, A. *et al.* The function of PML in p53-dependent apoptosis. *Nature Cell Biol.* **2,** 730–736 (2000).
3. Louria-Hayon, I. *et al.* PML protects p53 from Mdm2-mediated inhibition and degradation. *J. Biol. Chem.* **278,** 33134–33141 (2003).
4. Wei, X. *et al.* Physical and functional interactions between PML and MDM2. *J. Biol. Chem.* **278,** 29288–29297 (2003).
5. Zhu, H., Wu, L. & Maki, C. G. MDM2 and PML antagonize each other through their direct interaction with p53. *J. Biol. Chem.* **278,** 49286–49292 (2003).
6. Kurki, S., Latonen, L. & Laiho, M. Cellular stress and DNA damage invoke temporally distinct Mdm2, p53 and PML complexes and damage-specific nuclear relocalization. *J. Cell Sci.* **116,** 3917–3925 (2003).
7. Oren, M. Regulation of the p53 tumor suppressor protein. *J. Biol. Chem.* **274,** 36031–36034 (1999).
8. Weber, J. D., Taylor, L. J., Roussel, M. F., Sherr, C. J. & Bar-Sagi, D. Nucleolar Arf sequesters Mdm2 and activates p53. *Nature Cell Biol.* **1,** 20–26 (1999).
9. Lohrum, M. A., Ludwig, R. L., Kubbutat, M. H., Hanlon, M. & Vousden, K. H. Regulation of HDM2 activity by the ribosomal protein L11. *Cancer Cell* **3,** 577–587 (2003).
10. Salomoni, P. & Pandolfi, P. P. The role of PML in tumor suppression. *Cell* **108,** 165–170 (2002).
11. Jensen, K., Shiels, C. & Freemont, P. S. PML protein isoforms and the RBCC/TRIM motif. *Oncogene* **20,** 7223–7233 (2001).
12. Ferbeyre, G. *et al.* PML is induced by oncogenic *ras* and promotes premature senescence. *Genes Dev.* **14,** 2015–2027 (2000).
13. Fogal, V. *et al.* Regulation of p53 activity in nuclear bodies by a specific PML isoform. *EMBO J.* **19,** 6185–6195 (2000).
14. Rubbi, C. P. & Milner, J. Disruption of the nucleolus mediates stabilization of p53 in response to DNA damage and other stresses. *EMBO J.* **22,** 6068–6077 (2003).
15. Abraham, R. T. Cell-cycle-checkpoint signaling through the ATM and ATR kinases. *Genes Dev.* **15,** 2177–2196 (2001).
16. Sarkaria, J. N. *et al.* Inhibition of ATM and ATR kinase activities by the radiosensitizing agent, caffeine. *Cancer Res.* **59,** 4375–4382 (1999).
17. Gage, B. M. *et al.* Spontaneously immortalized cell lines obtained from adult *Atm*-null mice retain sensitivity to ionizing radiation and exhibit a mutational pattern suggestive of oxidative stress. *Oncogene* **20,** 4291–4297 (2001).
18. Cliby, W. A. *et al.* Overexpression of a kinase-inactive ATR protein causes sensitivity to DNA-damaging agents and defects in cell-cycle checkpoints. *EMBO J.* **17,** 159–169 (1998).
19. Nghiem, P., Park, P. K., Kim, Y., Vaziri, C. & Schreiber, S. L. ATR inhibition selectively sensitizes G1 checkpoint-deficient cells to lethal premature chromatin condensation. *Proc. Natl Acad. Sci. USA* **98,** 9092–9097 (2001).
20. Bischof O., Kirsh O., Pearson M., Itahana K., Pelicci P. P. & Dejean A. Deconstructing PML-induced premature senescence. *EMBO J.* **21,** 3358–3369 (2002).
21. Stott F. J. *et al.* The alternative product of the human CDKN2A locus, p14(ARF), participates in a regulatory feedback loop with p53 and MDM2. *EMBO J.* **17,** 5001–5014 (1998).
22. Zhang, Y. *et al.* Ribosomal protein L11 negatively regulates oncoprotein MDM2 and mediates a p53-dependent ribosomal-stress checkpoint pathway. *Mol. Cell. Biol.* **23,** 8902–8912 (2003).
23. Carbone, R., Pearson, M., Minucci, S. & Pelicci, P. G. PML NBs associate with the hMre11 complex and p53 at sites of irradiation-induced DNA damage. *Oncogene* **21,** 1633–1640 (2002).
24. Cliby, W. A., Lewis, K. A., Lilly, K. K. & Kaufmann, S. H. S phase and G2 arrests induced by topoisomerase I poisons are dependent on ATR kinase function. *J. Biol. Chem.* **277,** 1599–1606 (2002).
25. Yang, S., Kuo, C., Bisi, J. E. & Kim, M. K. PML-dependent apoptosis after DNA damage is regulated by the checkpoint kinase hCds1/Chk2. *Nature Cell Biol.* **4,** 865–870 (2002).
26. Gostissa, M., Hofmann, T. G., Will, H. & Del Sal, G. Regulation of p53 functions: let's meet at the nuclear bodies. *Curr. Opin. Cell Biol.* **15,** 351–357 (2003).
27. Bernardi, R. & Pandolfi, P. P. Role of PML and the PML-nuclear body in the control of programmed cell death. *Oncogene* **22,** 9048–9057 (2003).
28. Andersen, J. S. *et al.* Directed proteomic analysis of the human nucleolus. *Curr. Biol.* **12,** 1–11 (2002).